

Supporting Information (SI)

Efficient organic light-emitting diodes based on iridium(III) complexes containing indolo[3,2,1-*jk*]carbazole derivatives with narrow emission bandwidths and low efficiency roll offs

Xiang-Ji Liao,^{1#} Jin-Jun Zhu,^{1#} Li Yuan,¹ Zhi-Ping Yan,¹ Xu-Feng Luo,¹ Yi-Pin Zhang,¹ Jun-Jian Lu,¹ and You-Xuan Zheng^{1,2*}

¹State Key Laboratory of Coordination Chemistry, Jiangsu Key Laboratory of Advanced Organic Materials, School of Chemistry and Chemical Engineering, Nanjing University, Nanjing 210093, P. R. China. E-mail: yxzhang@nju.edu.cn.

²Shenzhen Research Institute of Nanjing University, Shenzhen 518057, P. R. China.

#Liao and Zhu have same contribution to this paper.

S1. General information

NMR measurements were conducted on a Bruker AM 400 spectrometer. High resolution electrospray mass spectra (HRMS) was measured on G6500 from Agilent for complexes. Absorption spectra were measured on a UV-3100 spectrophotometer and photoluminescence spectra were obtained from a Hitachi F-4600 photoluminescence spectrophotometer. Cyclic voltammetry measurements were conducted on a MPI-A multifunctional electrochemical and chemiluminescent system (Xi'an Remex Analytical Instrument Ltd. Co., China) at room temperature, with a polished Pt plate as the working electrode, platinum thread as the counter electrode and Ag-AgNO₃ (0.1 M) in CH₃CN as the reference electrode, tetra-*n*-butylammonium perchlorate (0.1 M) was used as the supporting electrolyte, using Fc⁺ /Fc as the internal standard, the scan rate was 0.1 V/s. The absolute photoluminescence quantum yields (Φ) and the decay lifetimes of the compounds was measured with HORIBA FL-3 fluorescence spectrometer. Thermogravimetric analysis (TGA) was performed on a Pyris 1 DSC under nitrogen at a heating rate of 10 °C min⁻¹. The single crystals of complexes were carried out on a Bruker SMART CCD diffractometer using monochromated Mo Ka radiation ($\lambda = 0.71073 \text{ \AA}$) at room temperature. Cell parameters were retrieved using SMART software and refined using SAINT on all observed reflections.

S2. OLEDs fabrication and measurement.

All OLEDs were fabricated on the pre-patterned ITO-coated glass substrate with a sheet resistance of 15 Ω sq⁻¹. The deposition rate for organic compounds is 1-2 Å s⁻¹. The phosphor and the host (2,6DCzPPy) was co-evaporated to form emitting layer from two separate sources. The cathode consisting of LiF / Al was deposited by evaporation of LiF with a deposition rate of 0.1 Å s⁻¹ and then by evaporation of Al metal with a rate of 3 Å s⁻¹.

The characteristic curves of the devices were measured with a computer which controlled KEITHLEY 2400 source meter with a calibrated silicon diode in air without device encapsulation. On the basis of the uncorrected PL and EL spectra, the Commission Internationale de l'Eclairage (CIE) coordinates were calculated using a test program of the Spectra scan PR650 spectrophotometer, The EQE of EL devices were calculated based on the photo energy measured by the photodiode.

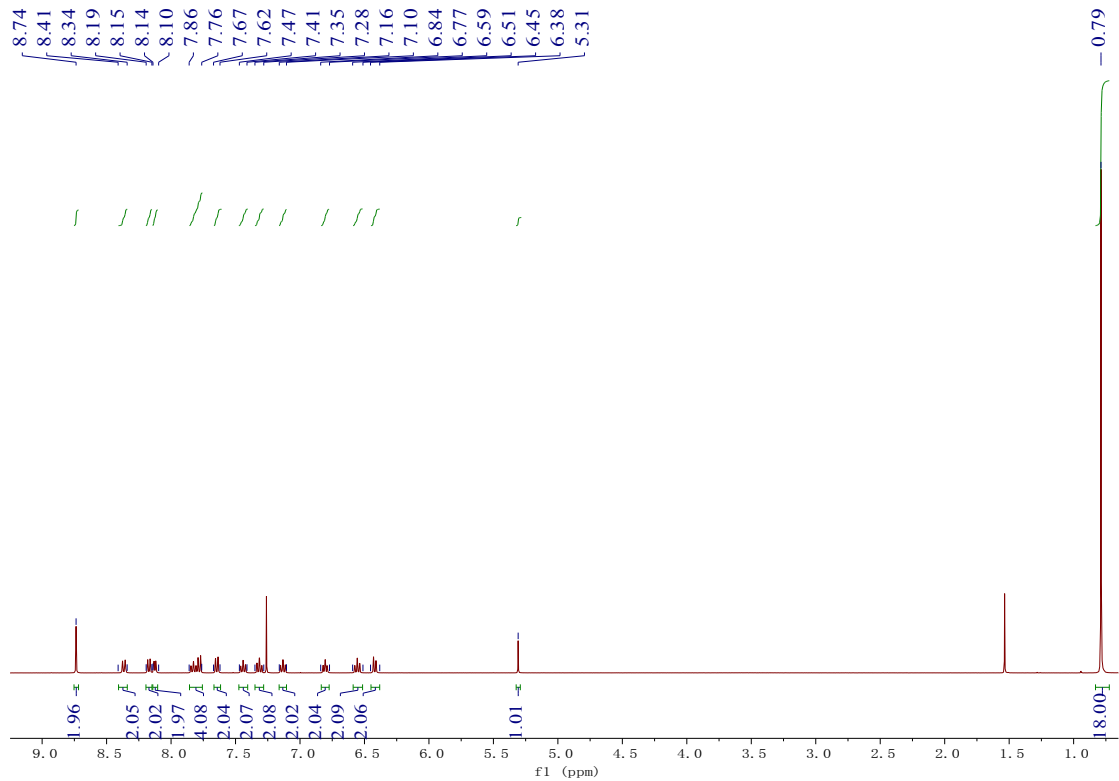


Fig. S1 ^1H NMR spectrum of (pyidcz) $_2\text{Ir}(\text{tmd})$ complex.

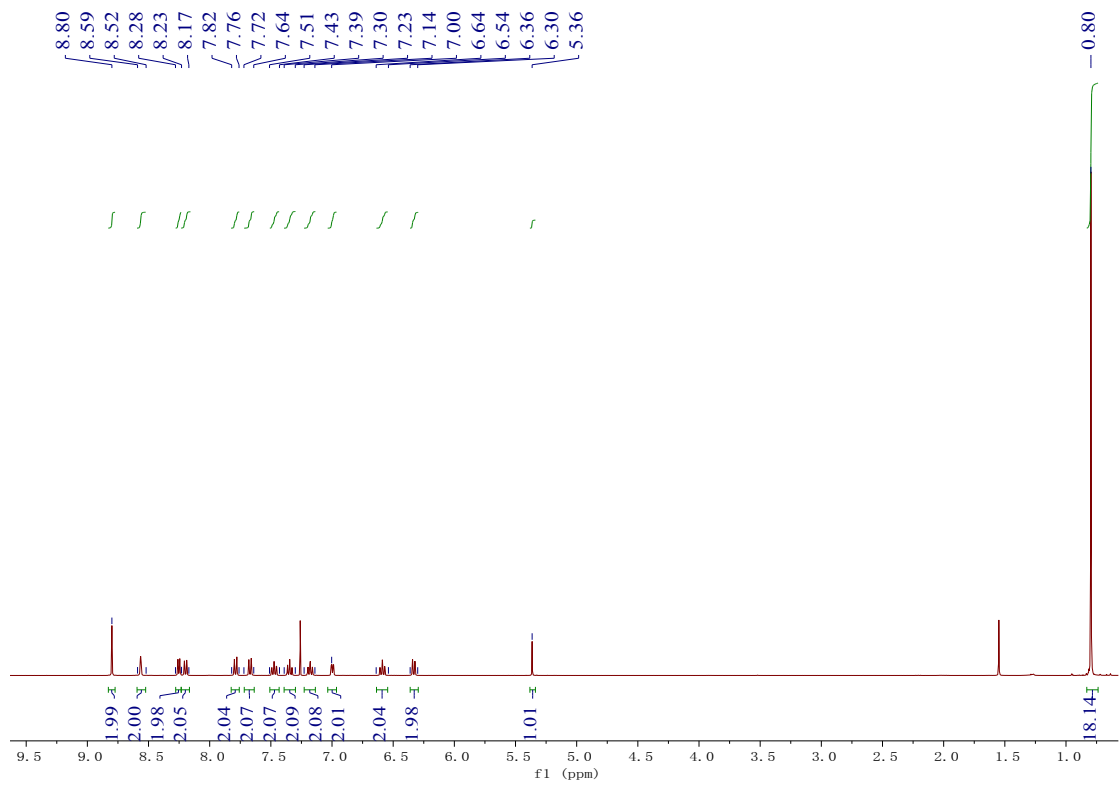


Fig. S2 ^1H NMR spectrum of $(\text{tfpyidcz})_2\text{Ir}(\text{tmd})$ complex.

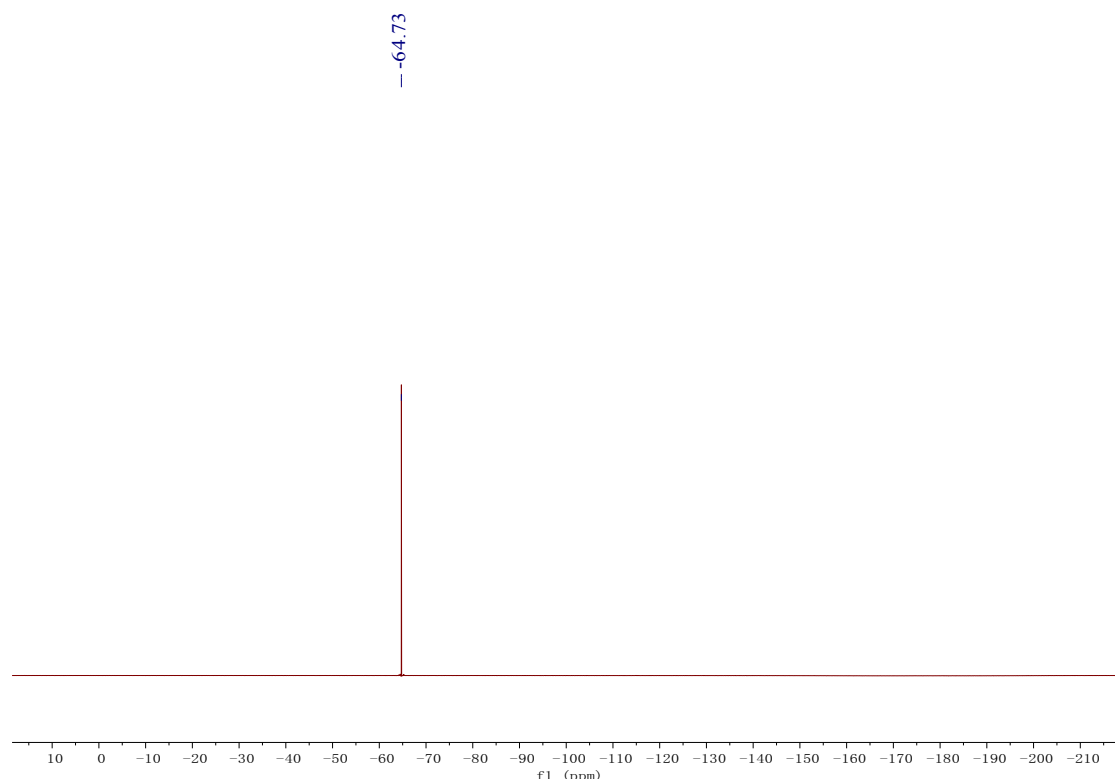


Fig. S3 ^{19}F NMR spectrum of $(\text{tfpyidcz})_2\text{Ir}(\text{tmd})$ complex.

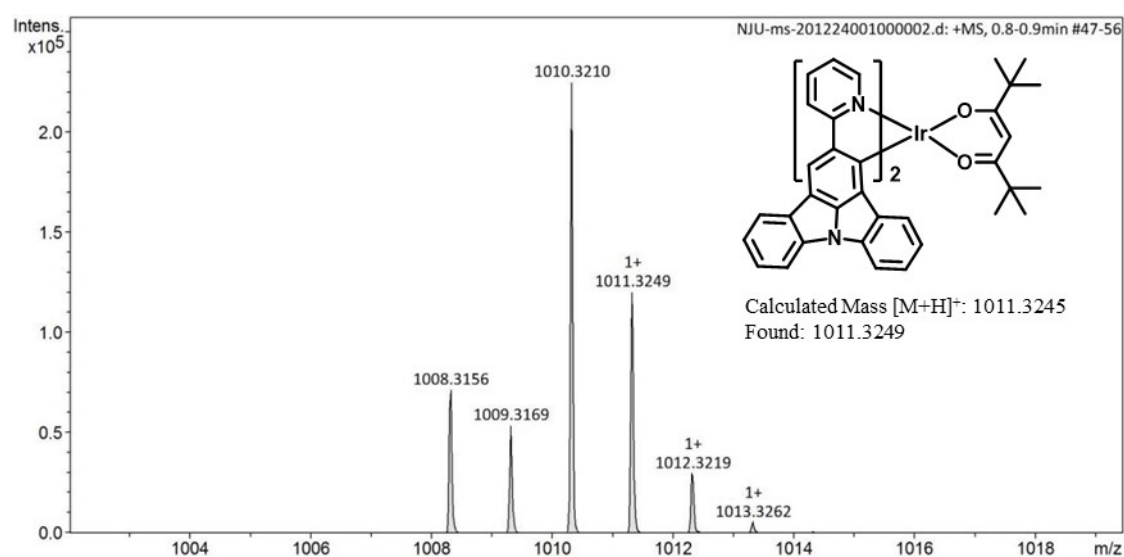


Fig. S4 HRMS spectrum of $(\text{pyidcz})_2\text{Ir}(\text{tmd})$ complex.

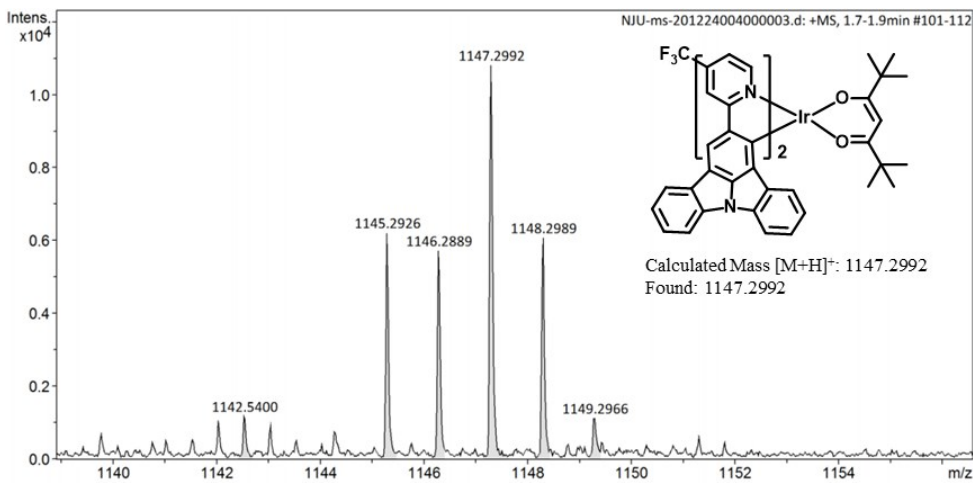


Fig. S5 HRMS spectrum of $(\text{tpyidcz})_2\text{Ir}(\text{tmd})$ complex.

Table S1. Crystal information of $(\text{pyidcz})_2\text{Ir}(\text{tmd})$ and $(\text{tfpyidcz})_2\text{Ir}(\text{tmd})$ complexes.

	$(\text{pyidcz})_2\text{Ir}(\text{tmd})$	$(\text{tfpyidcz})_2\text{Ir}(\text{tmd})$
Formula	$\text{C}_{57}\text{H}_{45}\text{IrN}_4\text{O}_2$	$\text{C}_{59}\text{H}_{43}\text{F}_6\text{IrN}_4\text{O}_2$
Formula weight	1010.17	1146.17
T (K)	189.99	192.99
Wavelength (Å)	1.34139	1.34139
Crystal system	Triclinic	Monoclinic
Space group	$P -1$	$P2_1/n$
a (Å)	13.4272(4)	15.4399(7)
b (Å)	19.5665(6)	19.6457(9)
c (Å)	19.8361(6)	18.3164(8)
α (deg)	66.9160(10)	90
β (deg)	82.6740(10)	102.973(2)
γ (deg)	71.3750(10)	90
V (Å ³)	4543.0(2)	5414.1(4)
Z	4	4
ρ_{calcd} (mg m ⁻³)	1.477	1.406
μ (Mo K α) (mm ⁻¹)	4.189	3.664
F (000)	2032	2288
Reflns collected	40573	35473
Unique	16116	9859
Data/restraints/params	16116/6/1165	9859 / 51 / 683
GOF on F^2	1.064	1.032
R_1^{a} , $wR_2^{\text{b}}[I > 2\sigma(I)]$	0.0598, 0.1424	0.0413, 0.1010
R_1^{a} , wR_2^{b} (all data)	0.0798, 0.1579	0.0548, 0.1089
CCDC NO	2052163	2052136

$R_1^{\text{a}} = \sum ||F_{\text{o}}| - |F_{\text{c}}|| / \sum |F_{\text{o}}|$. $wR_2^{\text{b}} = [\sum w(F_{\text{o}}^2 - F_{\text{c}}^2)^2 / \sum w(F_{\text{o}}^2)]^{1/2}$

Table S2. Selected bond lengths and angles of (pyidcz)₂Ir(tmd) complex.

Selected bonds (Å)			
Ir(01)-O(005)	2.143(5)	Ir(01)-N(007)	2.017(5)
Ir(01)-O(006)	2.115(5)	Ir(01)-N(008)	2.016(6)
Ir(01)-C(009)	1.989(7)	Ir(01)-C(00A)	1.979(6)
Ir(02)-O(003)	2.124(5)	Ir(02)-O(004)	2.122(4)
Ir(02)-N(00B)	2.008(7)	Ir(02)-N(00C)	2.025(7)
Ir(02)-C(00K)	1.992(7)	Ir(02)-C(012)	1.997(7)
Selected angles (°)			
O(006)-Ir(01)-O(005)	86.61(19)	N(007)-Ir(01)-O(005)	93.3(2)
N(007)-Ir(01)-O(006)	85.9(2)	N(008)-Ir(01)-O(005)	83.9(2)
N(008)-Ir(01)-O(006)	93.7(2)	N(008)-Ir(01)-N(007)	177.2(2)
C(009)-Ir(01)-O(005)	170.0(2)	C(009)-Ir(01)-O(006)	84.9(2)
C(009)-Ir(01)-N(007)	81.0(2)	C(009)-Ir(01)-N(008)	101.8(2)
C(00A)-Ir(01)-O(005)	88.1(2)	C(00A)-Ir(01)-O(006)	173.1(2)
C(00A)-Ir(01)-N(007)	98.9(2)	C(00A)-Ir(01)-N(008)	81.3(2)
C(00A)-Ir(01)-C(009)	100.7(3)	O(004)-Ir(02)-O(003)	87.41(19)
N(00B)-Ir(02)-O(003)	84.0(2)	N(00B)-Ir(02)-O(004)	92.2(2)
N(00B)-Ir(02)-N(00C)	174.4(2)	N(00C)-Ir(02)-O(003)	93.2(2)
N(00C)-Ir(02)-O(004)	82.8(2)	C(00K)-Ir(02)-O(003)	172.3(3)
C(00K)-Ir(02)-O(004)	87.5(2)	C(00K)-Ir(02)-N(00B)	101.9(3)
C(00K)-Ir(02)-N(00C)	80.5(3)	C(00K)-Ir(02)-C(012)	99.0(3)
C(012)-Ir(02)-O(003)	86.7(2)	C(012)-Ir(02)-O(004)	171.4(3)
C(012)-Ir(02)-N(00B)	81.0(3)	C(012)-Ir(02)-N(00C)	103.7(3)

Table S3. Selected bond lengths and angles of (tfipyidcz)₂Ir(tmd) complex.

Selected bonds (Å)			
Ir(01)-O(001)	2.141(3)	Ir(01)-O(002)	2.126(3)
Ir(01)-N(002)	2.011(3)	Ir(01)-N(004)	2.013(3)
Ir(01)-C(003)	1.989(4)	Ir(01)-C(004)	1.999(4)
Selected angles (°)			
O(002)-Ir(01)-O(001)	87.81(11)	N(002)-Ir(01)-O(001)	94.30(13)
N(002)-Ir(01)-O(002)	80.26(12)	N(002)-Ir(01)-N(004)	172.35(13)
N(004)-Ir(01)-O(001)	80.05(12)	N(004)-Ir(01)-O(002)	94.30(12)
C(003)-Ir(01)-O(001)	173.90(14)	C(003)-Ir(01)-O(002)	86.97(14)
C(003)-Ir(01)-N(002)	81.71(15)	C(003)-Ir(01)-N(004)	103.49(15)

C(003)-Ir(01)-C(004)	96.20(16)	C(004)-Ir(01)-O(001)	89.23(14)
C(004)-Ir(01)-O(002)	175.01(13)	C(004)-Ir(01)-N(002)	103.98(15)
C(004)-Ir(01)-N(004)	81.22(15)		

Table S4. HOMO and LUMO electron cloud density distributions of each fragment of two Ir(III) complexes.

Complex	Orbital	Energy/ eV	E_g/ eV	Composition (%)		
				Ir	Main ligand	Ancillary ligand
(pyidcz) ₂ Ir(tmd)	HOMO	-4.91	3.47	36.36	60.12	3.52
	LUMO	-1.44		3.39	93.45	3.16
(tfpyidcz) ₂ Ir(tmd)	HOMO	-5.27	2.70	31.44	65.20	3.35
	LUMO	-2.57		3.88	94.52	1.69

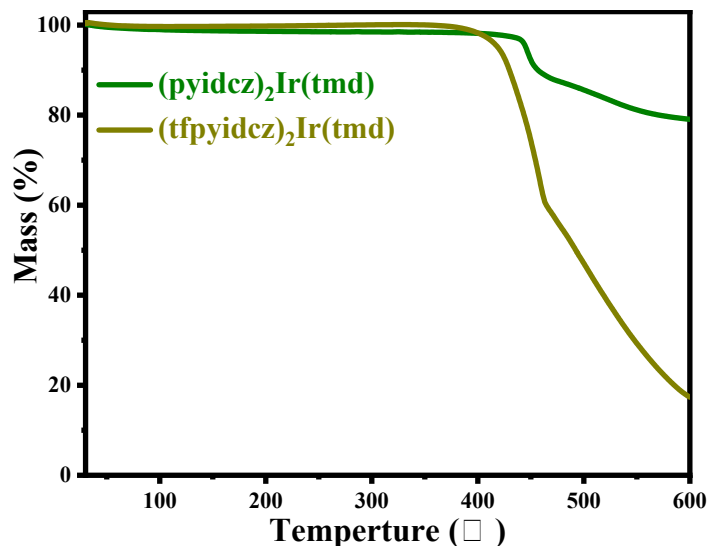


Fig. S6 TGA curves of $(\text{pyidcz})_2\text{Ir}(\text{tmd})$ and $(\text{tfpyidcz})_2\text{Ir}(\text{tmd})$ complexes.

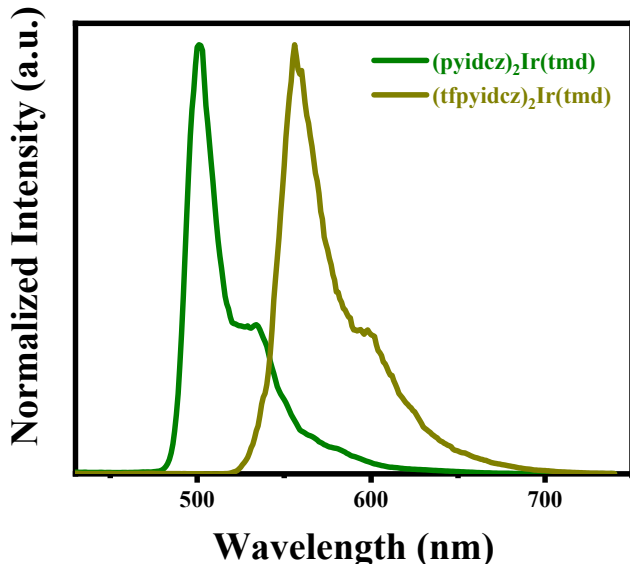


Fig. S7 The 77 K phosphorescent spectra of $(\text{pyidcz})_2\text{Ir}(\text{tmd})$ and $(\text{tfpyidcz})_2\text{Ir}(\text{tmd})$ in dilute DCM (10^{-5} M).

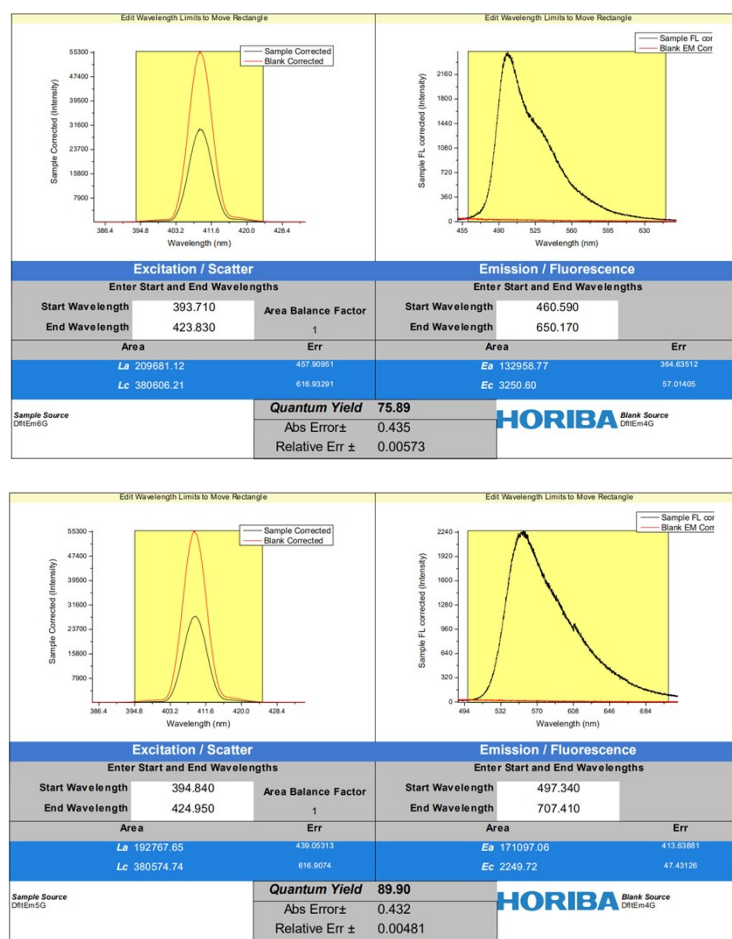


Fig. S8 The photoluminescence quantum yields of $(\text{pyidcz})_2\text{Ir}(\text{tmd})$ and $(\text{tfpyidcz})_2\text{Ir}(\text{tmd})$ in dilute DCM (10^{-5} M).

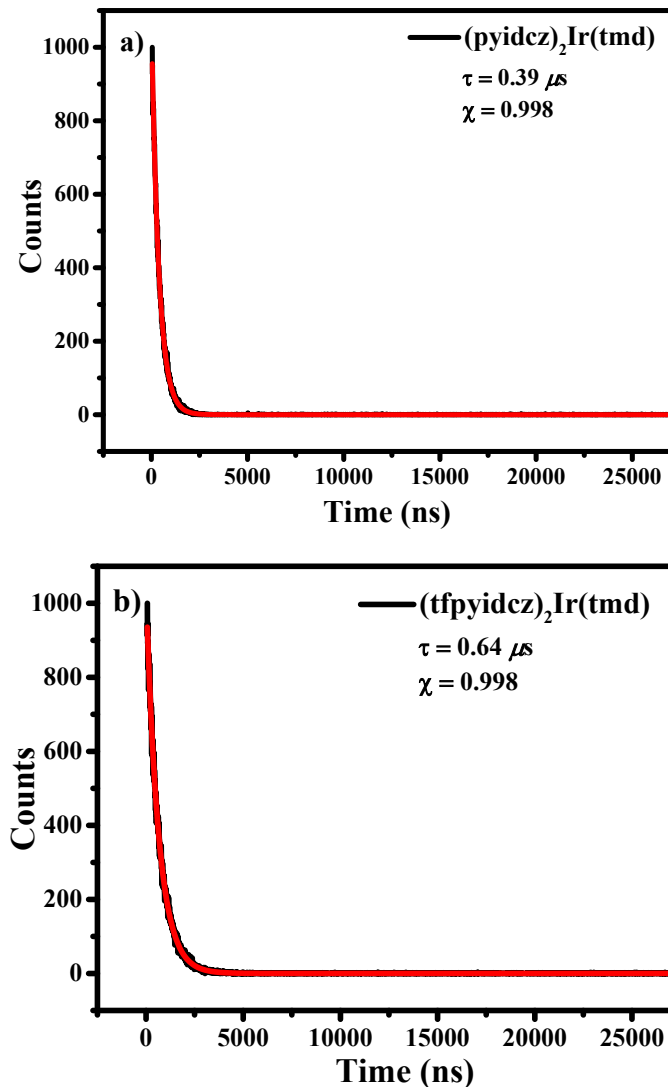


Fig. S9. Phosphorescence lifetime curves of the Ir(III) complexes in dilute DCM (10^{-5} M) at RT.

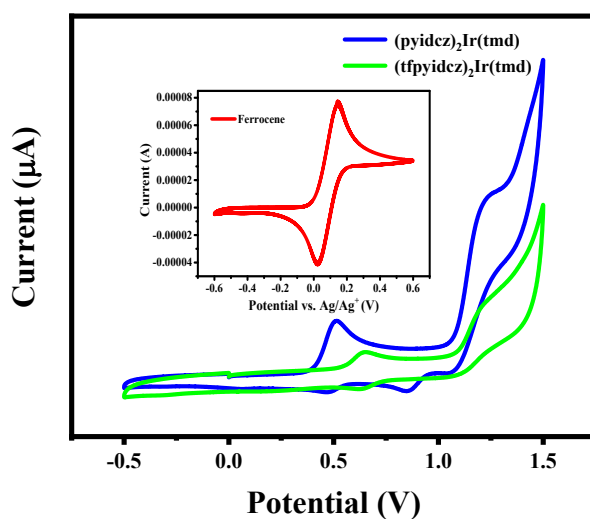


Fig. S10 Cyclic voltammetry curves of $(\text{pyidcz})_2\text{Ir}(\text{tmd})$ and $(\text{tfpyidcz})_2\text{Ir}(\text{tmd})$ in acetonitrile with ferrocene as the internal standard.